


# GPR4 in the pH-dependent migration of melanoma cells in the tumor microenvironment

Judith Anthea Stolwijk<sup>1,2</sup> | Susanne Wallner<sup>1</sup> | Judith Heider<sup>1</sup> | Bernadett Kurz<sup>1</sup> | Lisa Pütz<sup>2</sup> | Stefanie Michaelis<sup>2,3</sup> | Barbara Goricnik<sup>2</sup> | Julia Erl<sup>2</sup> | Linda Frank<sup>2</sup> | Mark Berneburg<sup>1</sup> | Frank Haubner<sup>4</sup> | Joachim Wegener<sup>2,3</sup> | Stephan Schreml<sup>1</sup> 

<sup>1</sup>Department of Dermatology, University Medical Center Regensburg, Regensburg, Germany

<sup>2</sup>Faculty of Chemistry and Pharmacy, Institute of Analytical Chemistry, Chemo- and Biosensors, University of Regensburg, Regensburg, Germany

<sup>3</sup>Fraunhofer Research Institution for Microsystems and Solid State Technologies EMFT, Regensburg, Germany

<sup>4</sup>Department of Otorhinolaryngology, Ludwig Maximilians University Munich, Munich, Germany

## Correspondence

Judith Anthea Stolwijk and Stephan Schreml, Department of Dermatology, University Medical Center Regensburg, Franz-Josef-Strauß-Allee 11, 93053 Regensburg, Germany.  
Email: [judith.stolwijk@ur.de](mailto:judith.stolwijk@ur.de) and [stephan.schreml@ukr.de](mailto:stephan.schreml@ukr.de)

## Funding information

Deutsche Forschungsgemeinschaft

## Abstract

Due to its high metastatic potential, malignant melanoma is one of the deadliest skin cancers. In melanoma as well as in other cancers, acidification of the tumor microenvironment (=TME, inverse pH-gradient) is a well-known driver of tumor progression and metastasis. Membrane-bound receptors, such as the proton-sensitive GPCR (pH-GPCR) GPR4, are considered as potential initiators of the signalling cascades relevant to malignant transformation. In this study, we investigated the pH-dependent migration of GPR4 wildtype/overexpressing SK-Mel-28 cells using an impedance-based electrical wounding and migration assay and classical Boyden chamber experiments. Migration of GPR4 overexpressing SK-Mel-28 cells was enhanced in a range of pH 6.5–7.5 as compared to controls in the impedance-based electrical wounding and migration assay. In Boyden chamber experiments, GPR4 overexpression only increased migration at pH 7.5 in a Matrigel-free setup, but not at pH 6.5. Results indicate that GPR4 is involved in the migration of melanoma cells, especially in the tumor periphery, and that this process is affected by pH in the TME.

## KEYWORDS

Boyden chamber, ECIS, GPR4, impedance, malignant melanoma, migration, pH-GPCR

## 1 | INTRODUCTION

Malignant melanoma is one of the most aggressive and deadliest forms of skin cancer, which is mainly attributed to a high metastatic potential of melanoma cells.<sup>1–3</sup> A central hallmark of solid tumors, such as malignant melanoma, is the acidification of the microenvironment represented by the extracellular pH ( $pH_e$ ).<sup>1,4,5</sup> The  $pH_e$  of solid tumor cells is usually more acidic ( $pH_e$  5.9–7.0) than the extracellular environment of healthy tissue ( $pH_e$  7.3–7.4).<sup>4</sup> This is due to hypoxia, metabolic changes (Waarburg effect) and a plethora of membrane-bound

channels/transporters (NHE1, carboanhydrases, monocarboxylate transporters, bicarbonate symporters and V-ATPases), which regulate  $pH_e$ .<sup>5–7</sup> An acidic extracellular environment promotes characteristic tumor cell behaviour, such as increased proliferation, migration and invasion, as well as changes in the immune response. The molecular response of cells to altered  $pH_e$  (inverse/inside-out pH gradient) are mediated by different intracellular and extracellular sensors including proton-sensitive G-protein coupled receptors (pH-GPCRs).<sup>5,8</sup>

The four pH-GPCRs GPR4 (GPR19), GPR65 (TDAG8, T-cell death-associated gene 8), GPR68 (OGR1, ovarian cancer GPCR 1)

This is an open access article under the terms of the [Creative Commons Attribution-NonCommercial-NoDerivs](https://creativecommons.org/licenses/by-nc-nd/4.0/) License, which permits use and distribution in any medium, provided the original work is properly cited, the use is non-commercial and no modifications or adaptations are made.

© 2022 The Authors. *Experimental Dermatology* published by John Wiley & Sons Ltd.

and GPR132 (G2A, G2 accumulation protein) are activated by a decrease in extracellular pH ( $pH_e$ ) via protonation of different histidine residues on the extracellular surface of the pH-GPCRs,<sup>9-11</sup> as well as potential additional acidic residues buried further inside the receptors.<sup>12</sup> pH-GPCRs have been shown to be involved in tumor cell proliferation, apoptosis, metastasis, angiogenesis, modulation of inflammation and immune responses, and therefore are recognized as potential players in cancer progression.<sup>9,10,13-18</sup> For example, GPR4 activation by an acidic environment was shown to influence inflammatory processes, cell migration and angiogenesis in different cell types, including vascular endothelial cells.<sup>13-15,18</sup>

While a number of studies suggest that GPR68 serves as a metastasis suppressor in different cancer types,<sup>19-22</sup> GPR65 and GPR132 are predominantly associated with functions in immune and blood-borne cells.<sup>23-26</sup> The role of GPR4 in cancer progression is less clear, as tumor-suppressing, as well as cancer-promoting effects, have been identified in different cancer cell types and disease models.<sup>18,27-31</sup> Ectopic overexpression of GPR4 in B16F10 melanoma cells inhibited their migration in an acidic environment and reduced their potential to form lung metastases in a mouse model.<sup>13</sup> GPR4 decreased cell spreading and affected focal adhesion localization, which points to alterations in cell mobility.<sup>28</sup> Especially at low pH the GPR4 overexpressing cells rounded up and exhibited less dynamic focal adhesions at cell edges.<sup>28</sup> In a model with GPR4-deficient mice tumor growth was strongly reduced in two orthotopic models with 4T1 breast tumor cells or CT26 colon tumor cells, likely mediated via a reduced angiogenic response to VEGF.<sup>18</sup>

Overexpression of GPR4 in squamous cell carcinoma of the head and neck was shown to lead to an increased expression and secretion of IL6, IL8 and VEGF under acidic conditions.<sup>27</sup> In a vascularization model, GPR4 overexpressing cancer cells showed increased recruitment of new blood vessels under acidic conditions.<sup>27</sup> In this line, also a study with colorectal cancer cells supports the cancer-promoting effect of GPR4.<sup>30</sup> The knockdown of GPR4 in HCT116 and HT29 colorectal cancer cell lines resulted in suppressed growth and in significantly inhibited migration. It was found that GPR4 was upregulated in human colorectal cancer samples and that high expression correlated with late-stage tumors and poor survival rate.<sup>30</sup> Another quantitative real-time PCR screen of total RNA samples extracted from a panel of human primary tumors revealed that GPR4 was overexpressed more than fivefold over normal tissue controls in a significant portion of the breast, ovarian, colon, liver and kidney tumors.<sup>29</sup> The study showed that overexpression of GPR4 in NIH3T3 or HEK293 cells malignantly transformed the cells. Overexpression of GPR4 in HEK293 cells led to transcriptional activation of SRE and CRE promoter-driven genes, indicating that multiple signalling cascades including mitogenic pathways are potentially activated by GPR4. NIH3T3 cells overexpressing GPR4 and injected into mice led to increased tumor formation.<sup>29</sup>

We recently found that pH-GPCRs are differentially expressed in many skin cancers.<sup>32,33</sup> GPR4 was expressed with high scores in tumor tissue of Merkel cell carcinoma, and especially malignant melanoma.<sup>32,33</sup> Tissue microarray analysis moreover

revealed that all 4 pH-GPCRs are particularly highly expressed in malignant melanoma.<sup>32</sup> Interestingly, there was increased dermal expression of GPR4 compared to benign nevus cell nevi, indicating a possible role of GPR4 in tumor cell migration and possibly malignant transformation. Therefore, in this study, we focused on the role of GPR4 in malignant melanoma. We investigated the migration of GPR4 overexpressing SK-Mel-28 malignant melanoma cells compared to control cells using an impedance-based electrical wounding and migration assay paralleled by Boyden chamber experiments.

## 2 | METHODS

### 2.1 | Cell culture

SK-Mel-28 melanoma cells were purchased from CLS (#300 337). Cells were grown in DMEM (Sigma-Aldrich, D5671) supplemented with 10% fetal calf serum (FCS) (Biochrom), 1% L-glutamine (L-Glu) (Sigma-Aldrich) and 1% penicillin/streptomycin (P/S) (Sigma-Aldrich) in a standard humidified cell culture incubator with 5% CO<sub>2</sub>.

### 2.2 | pH-media

To create a defined  $pH_e$  the bicarbonate-free, KH<sub>2</sub>PO<sub>4</sub>- and Na<sub>2</sub>HPO<sub>4</sub>-buffered Leibowitz' (L15) medium (Fisher Thermo Scientific, 21083-027) supplemented with 10% FCS and 1% P/S, was adjusted to different pH. The different pH of the L15 media (6.0, 6.5, 6.75, 7.0, 7.25, 7.5, 8.0 and 8.5) were adjusted by adding NaH<sub>2</sub>PO<sub>4</sub> (Sigma-Aldrich) and/or K<sub>3</sub>PO<sub>4</sub> (Fluka) until the respective pH was reached as measured with a pH-meter (Hanna Instruments). The L15 media were sterile filtered through a 0.2  $\mu$ m filter (Sarsted, Filtropur S, PES, 20003477). Carbonate-free pH-buffered media were used at ambient CO<sub>2</sub> conditions (incubator set to 0% CO<sub>2</sub> or the presence of CO<sub>2</sub>) was excluded by use of hermetically sealed 7 L rectangular containers (Mitsubishi Gas Chemical).

### 2.3 | Impedance assay

To study the migration of SK-Mel-28 cells we use an impedance-based automated wound healing assay that is based on the work published by Wegener et al.<sup>34</sup> The original assay was optimized to study melanoma cell migration in a 96-well format (Figure 1). The assay relies on seeding the cells to confluence on thin, planar gold-film electrodes deposited on the bottom foil of a 96-well plate (96W1E<sup>+</sup>, Applied BioPhysics Inc.). The electrodes can be used for both, for non-invasive measurements to detect electrode coverage with cells, and for the application of invasive electric wounding pulses to create a defined lesion within the cell layer. Cell coverage of the electrodes is monitored by non-invasive impedance readings as described in detail elsewhere.<sup>35,36</sup> In brief, as the adherent cells

act like insulating particles, they block free current flow and therefore increase the impedance compared to a cell-free electrode. With increasing cell coverage of the electrodes with cells the impedance increases. The alternating current amplitudes that are applied for impedance measurements are weak and non-invasive.<sup>36</sup> However, when AC current pulses of higher amplitude are injected (2800  $\mu$ A, 32 kHz, 60 s), the cells on the small electrode are killed by irreversible membrane damage. Cell damage is strictly limited to the cells on the active electrode area while surrounding cells remain unharmed. After the electric wounding pulse is turned off, the viable cells in the periphery of the electrode can migrate into the lesion. This repopulation of the electrode is monitored by non-invasive impedance measurements.

In our assay, SK-Mel-28 melanoma cells were seeded to the wells of an ECIS 96-well plate (96W1E<sup>+</sup>, Applied Biophysics Inc., see schematic drawing in [Figure 1A](#)) at a density of 150 000 cells/cm<sup>2</sup> in DMEM supplemented with FCS and P/S. The entire adhesion and cell layer formation process was monitored by non-invasive impedance measurements using the ECIS Z $\theta$  instrument equipped with a 96-well array holder station, personal computer and software (Applied BioPhysics Inc.). Impedance was measured at 4, 12, 40 and 64 kHz. Impedance data versus time in hours (t/h) were plotted for 40 kHz as this is a typical frequency for monitoring electrode coverage with cells.<sup>34,36</sup> Cells were seeded to the electrodes after recording an initial baseline in a medium for 30–60 min. To do so the data acquisition was paused, the plate was removed from the 96-well holder station and initially suspended cells were seeded. After placing the plate back in the 96-well older station the measurement was resumed. Cells were allowed to settle to the electrode for 2 h before the measurement was paused again to exchange the complete medium for L15 with different pH<sub>e</sub> (see Chapter 2.2). The incubator CO<sub>2</sub> was set to 0% to maintain the according pH<sub>e</sub> in the carbonate-free media. The 96-well electrode array was reconnected to the ECIS instrument and after one impedance measurement cycle per well the cells on the electrodes were electrically wounded using the elevated field mode (EFM) of the ECIS instrument, applying a short, invasive electric pulse (32 kHz, 2800  $\mu$ A, 60 s) to the electrodes. Afterwards, non-invasive impedance measurement was resumed to monitor the cells' response to the wounding pulse and the repopulation of the electrode by intact cells. The efficiency of cell layer recovery by unwounded cells migrating inward from the periphery was quantified by calculating the area under the curve (AUC) of time course impedance data by integration. We chose a time frame of 24 h starting after the wounding pulse has been applied. The value of AUC (given in units of h<sup>2</sup>k $\Omega$ ) is higher for conditions in which the cells repopulate the electrode quickly and completely. Incomplete and slow recovery results in a low AUC.

## 2.4 | LIVE/DEAD assay and confocal microscopy

To document the success of electrical wounding along the impedance-based electrical wounding and migration assay the cell

layers were stained using a LIVE/DEAD Viability/Cytotoxicity Kit (Thermo Fisher Scientific Inc). Green fluorescent calcein stains live cells after the acetoxy-moiety of calcein-AM (CaAM) is cleaved by intracellular esterases. Ethidium-homodimer-1 (EthD-1) intercalates to the DNA of dead cells that have a compromised cell membrane. The staining solution contained 4  $\mu$ M EthD-1 and 2  $\mu$ M in CaAM in phosphate-buffered saline with calcium and magnesium (PBS<sup>++</sup>, Sigma-Aldrich, 806552). To stain the cells on the bottom of the 96W1E<sup>+</sup> array, the bottom foil that is glued to the 96-well scaffold was carefully peeled off and placed inside the lid of the plate that was used as a tray for staining. The cell layers were carefully submerged in a staining solution and incubated for 45 min in the dark at 0% CO<sub>2</sub> and 37°C. After the staining solution had been removed, cells were carefully washed twice with PBS<sup>++</sup>. After staining cells were examined in PBS<sup>++</sup> buffer using a confocal laser scanning microscope (Nikon Eclipse 90i) with a 10 $\times$  magnification objective. CaAM was excited at 488 nm and emission was detected using a 515/30 nm detector. EthD-1 was excited at 543 nm and emission was recorded with a 650 LP detector.

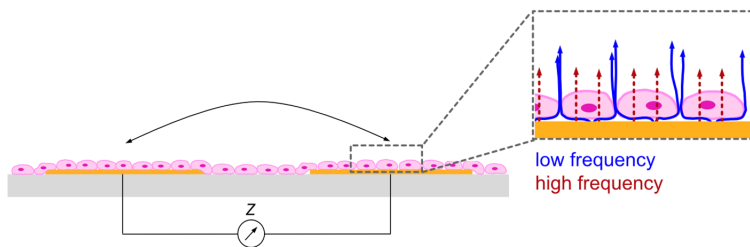
## 2.5 | Transfection

To create SK-Mel-28 melanoma cells stably expressing the pH-GPCR GPR4, cells were transfected with Lipofectamine 3000 (Invitrogen) with the pCMV6-AC-GFP-based expression plasmid GPR4 (NM\_005282) Human Tagged ORF Clone (OriGene technologies, RG209686). Cells were selected by 1 mg/ml Neomycin (G418). SK-Mel-28 wildtype (WT) cells of similar passage number as GPR4 overexpressing cells served as control. An effect of transfection with Lipofectamine on the migration of SK-Mel-28 cells was excluded (see [Figure S1](#)). Green fluorescence of stably transfected SK-Mel-28\_GPR4 cells (GPR4 was expressed as a chimeric protein to GFP) was inspected using a 60 $\times$  water immersion objective, excitation at 488 nm and 515/30 nm detection. All functional assays were performed without G418.

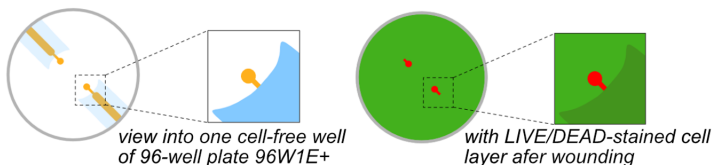
## 2.6 | qPCR

For mRNA isolation, cells from confluent monolayers in 75 cm<sup>2</sup> cell culture flasks were collected and seeded to a new 75 cm<sup>2</sup> cell culture flask after 1:10 dilution. Cells were grown to ~70%–80% confluence before they were harvested by trypsination and washed once by PBS. Total RNA was isolated using NucleoSpin RNA (Machery-Nagel, 740955.250). RNA concentration was determined by photometry using the NanoDrop instrument (Thermo Fisher Scientific). One microgram of total RNA was used to synthesize cDNA with the SuperScript II reverse transcriptase (Invitrogen, 18064014), dNTPs from NEB (N0446S) and Oligo DT primer from Roche (11034731001). The qPCR primers used to amplify the GPR4 gene segment were purchased from Microsynth and are listed in [Table 1](#). Forty-five cycles were performed at an annealing temperature of 60°C using Fast

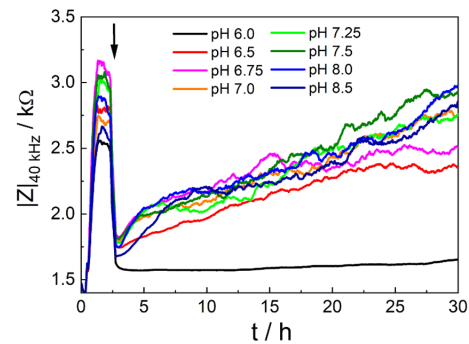
(A) side view



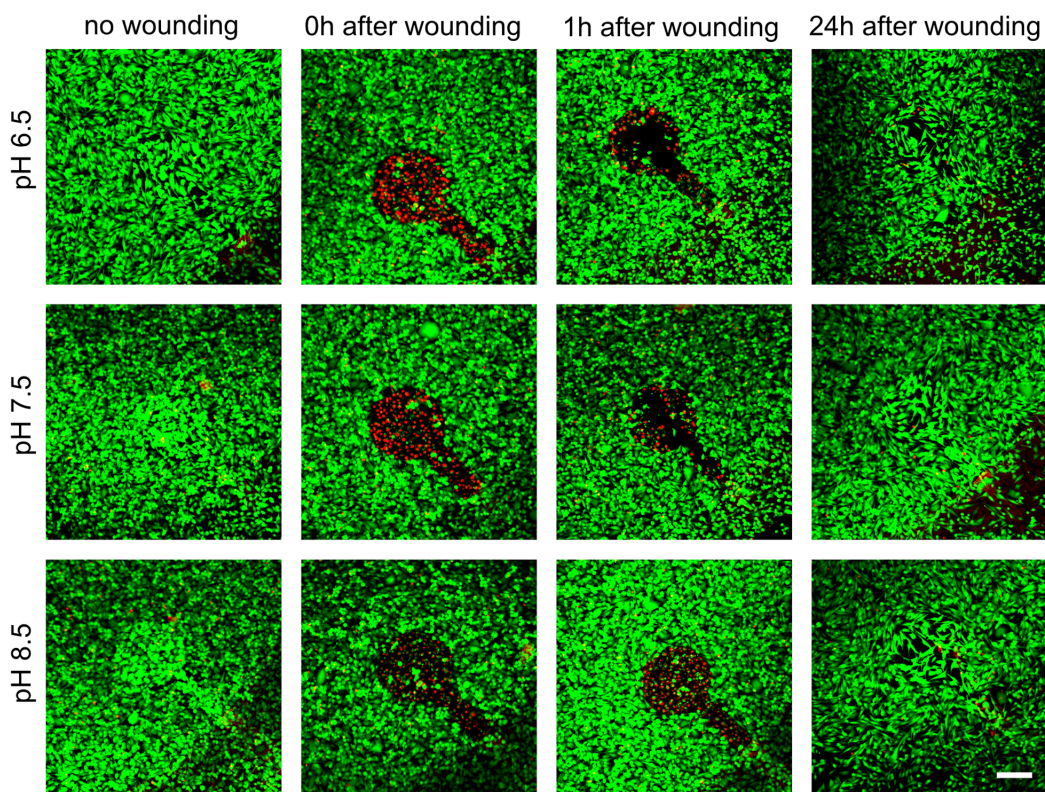
top view



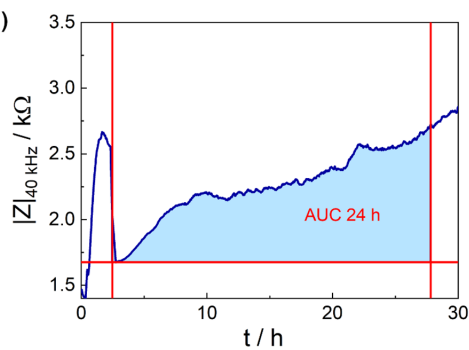
(B)



(C)



(D)



(E)

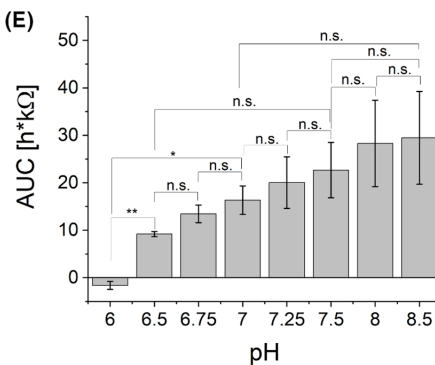




**FIGURE 1** Impedance-based electrical wounding and migration assay. (A) Schematic illustration of the assay principle. Cells are grown on a pair of coplanar electrodes patterned to the bottom of 96-well plates (96W1E<sup>+</sup>, Applied BioPhysics Inc.) as shown in the side view and top view. The zoom-in illustration of the side view indicates the current flow across the cell layer via the paracellular (blue arrows) and transcellular route (red arrows) at low and high AC frequencies, respectively. Electrical connection between the electrodes for cell monitoring and electrical wounding is provided by the ECIS instrument and the medium above the cell layer that serves as an electrolyte. The top view shows (left) the orientation of electrodes in a well that are partially passivated by an insulating polymer layer (blue) and (right) schematically illustrates a cell layer after electrical wounding and LIVE/DEAD staining (red: dead cells on the electrode, green: live cells in areas surrounding the electrodes). (B) Time course of impedance magnitude of the impedance-based electrical wounding and migration assay for SK-Mel-28 cells wounded in the presence of different pH<sub>e</sub> (6.0, 6.5, 6.75, 7.0, 7.25, 7.5, 8.0 and 8.5). At the time point indicated by the arrow, data acquisition was briefly paused for electric wounding of the cells on the electrode by an electric pulse of 32 kHz, 2800 μA, 60 s. (C) Confocal fluorescent micrographs (CLSM) of SK-Mel-28 cells on 96W1E<sup>+</sup> electrodes after LIVE/DEAD staining. Except for the controls in the left column (no wounding), cells were wounded as described in (B) in the presence of L15 media of pH 6.5, pH 7.5 or pH 8.5. Cells were subjected to staining and confocal fluorescent microscopy immediately after wounding (0 h), 1 h or 24 h after wounding. Scale bars represent 200 μm. (D) Principle of the area under the curve (AUC) calculation. The integral of the curve between the last timepoint before wounding and the time point 24 h after wounding are determined by OriginPro software analysis. The minimum impedance after electric wounding was used as the baseline for the calculation of the AUC. (E) Results of AUC determination for three individual experiments as shown in (B). The bar graph show AUC as mean ± SEM of N = 3(3) at different pH<sub>e</sub>.

**TABLE 1** qPCR primers

| Gene    | Primer     | Sequence                             | Efficiency |
|---------|------------|--------------------------------------|------------|
| GPR4    | GPR4_For   | 5'-CCG CTA CAA CCA<br>CAC CTT CT-3'  | 1.96       |
|         | GPR4_Rev   | 5'-CCA CGA ACA CCC<br>GAT AGA GG -3' |            |
| β-Actin | βActin_For | 5'-GCA TGG AGT CCT<br>GTG GCA TC-3'  | 1.89       |
|         | βActin_Rev | 5'-TTC TGC ATC CTG<br>TCG GCA AT-3'  |            |

Start Essential DNA Green Master (Roche, 06402712001) and the Roche LightCycler® 96 instrument (Roche). Primer efficiency and relative expression of GPR4 to β-actin, normalized to the WT control, were determined using the Roche LightCycler® 96 instrument software (Roche).

## 2.7 | Western blot

We used a stain-free blot approach, where the whole protein is quantifiable by the reaction with internal tryptophane. Thereby difficulties by membrane stripping and antibody interference can be avoided. For quantification, the ratio of the intensity from the GPR4 antibody to the intensity of the stainfree bands was taken. For Western Blot analysis cells were collected from 75 cm<sup>2</sup> cell culture flasks and seeded to a new 75 cm<sup>2</sup> cell culture flask after 1:10 dilution. Cells were grown to ~70%–80% confluence before they were harvested by trypsination. Cell pellets were washed with PBS and resuspended in RIPA buffer for protein extraction. Protein concentration was determined using a BCA protein assay kit (Pierce). Before loading the stain-free gel (Mini-PROTEAN TGX Stain-Free Precast Gel for any kD, Bio-Rad), 2 μg/μl protein in modified Laemmli buffer (Bio-Rad) with 25% DTT (Sigma-Aldrich) were denatured at 70°C for 10 min in modified Laemmli buffer (Bio-Rad) with 25% DTT

(Sigma-Aldrich). Proteins (10 μg per lane) were separated by sodium dodecyl sulfate-polyacrylamide gel electrophoresis and then transferred onto polyvinylidene fluoride membranes. Membranes were blocked with goat serum (10%, Merck) in PBS with 0.5% Tween-20 (PBST) for 2 h before incubation with anti-GPR4 antibody (Alomone Labs, Anti-GPR4 (extracellular) Antibody, #AGR-041, 1:1000) in 4% goat serum in PBST overnight at 4°C. The membranes were washed three times in PBST and were afterwards incubated with StarBright 700 Blue goat anti-rabbit IgG secondary antibody (Bio-Rad, #12004161, 1:10000) in 5% goat serum in PBST for 1 h at room temperature. After the membrane was washed three times with PBST, the immunoreactivity was detected by fluorescence detection (ChemiDoc, Bio-Rad). Densitometry of GPR4-positive fluorescence bands and referencing to whole protein content as imaged by stain-free technology (Bio-Rad, proprietary trihalo compound in stain-free gels) was performed using the Quantity One Software (Bio-Rad).

## 2.8 | Boyden chamber

Boyden chamber assays were performed using transparent PET porous membrane inserts with 8 μm pores (Omnilab, FALC353097) for 24-well plates in two variants: (i) without Matrigel, or (ii) with Matrigel. (i) In the assay without Matrigel 50000 cells/well were suspended in 200 μl serum-free L15 medium (L15, 1% P/S, pH 7.5), and applied to the top compartment of a trans-well insert with 8 μm membrane pores. As a chemoattractant, 500 μl complete L15 medium with 20% FCS (pH 7.5) was used in the lower compartment. Cells were allowed to migrate for 18 h in a humidified incubator at 37°C with 0% CO<sub>2</sub>. Following migration, cells in the upper chamber were removed using a cotton swab. The cells that had migrated to the other side of the membrane were fixed with 70% ethanol for 15 min and let dry for 15 min at RT. Afterwards, cells were stained with a 0.5% crystal violet solution in distilled water. The membranes were removed from the filter insert using a scalpel and embedded using the Roti-Histokitt II (ROTH, T160.1). Per filter, four different fields of view were counted

using a 10× objective of an inverted microscope. Cells were manually counted using the multipoint tool of the image analysis software ImageJ. (ii) To resemble invasion and thus 3D migration through the extracellular matrix a layer of Matrigel (Corning, 354234) was coated to 8 µm pore filters. Per membrane insert 100 µl of Matrigel diluted to a concentration of 400 µg/ml with ice-cold Dulbecco's PBS (DPBS, 1x, Gibco, 14190-144) to a concentration of 400 µg/ml was applied evenly to the top of each trans-well. Matrigel was allowed to solidify for 2 h at 37°C to form a thin gel layer. Afterwards, 50 000 cells in 200 µl serum-free L15 medium (pH 7.5) were added to each insert. A 500 µl of 20%-FCS containing L15 (pH 7.5) was applied to the bottom of the trans-well and cells were allowed to invade. Following invasion, the Matrigel was removed, and the cells were fixed, stained, and counted as described above.

## 2.9 | Statistical analysis

Experiments were performed in biological replicates and technical replicates. While each biological replicate represents a new batch of cells, the technical replicates are replicates within one experiment performed with the same batch of cells. Therefore, the number of experiments is presented as follows  $N = \text{total number of biological replicates (total number of technical replicates)}$ , for example,  $N = 3(6)$ . Data in bar graphs are shown as mean ± standard error of the mean (SEM). Data were subjected to a Shapiro-Wilk test for normality to ensure a normal distribution (0.01 level) (Origin 2021 software). Data with normal distribution were subjected to a two-sample *t*-test for comparison of means at the significance levels set to 0.05 or 0.01 (Origin 2021 software). ANOVA analysis was used where more than two samples were compared to each other (Origin 2021 software). Significance levels were indicated by asterisks: \* $p < 0.05$ , \*\* $p < 0.01$ , n.s. means data is not significantly different ( $p\text{-value} \geq 0.05$ ).

## 3 | RESULTS

In our recent publication, we reported on the increased expression of pH-GPCRs in tumor tissue of malignant melanoma.<sup>32</sup> Immunohistochemistry data indicated that GPR4 is more frequently expressed at high levels in malignant melanoma compared to benign nevus cell nevi, especially in the dermal portion of the skin. This increased dermal occurrence of GPR4 suggests that GPR4 promotes the migratory potential of melanoma cells which contributes to the formation of metastases. Therefore, we sought to investigate the role of GPR4 in the migration of SK-Mel-28 melanoma cells.

To measure the migration of SK-Mel-28 cells in a  $pH_e$ -dependent fashion, the impedance-based electrical wounding and migration assay was performed at different  $pH_e$  between pH 6.0 and pH 8.5 (Figure 1B). The time course of impedance at 40 kHz is shown for a typical wounding assay with SK-Mel-28 cells in the presence of different pH media (Figure 1B). Immediately after wounding, the impedance drops close to values close to those of a cell-free electrode.

Over time, as a result of cell migration from the electrode periphery, the impedance recovers to prepulse values or remains below, depending on the impact of the respective  $pH_e$  on cell migration.

The LIVE/DEAD assay results show that the electrical wounding of SK-Mel-28 cells was successful for different  $pH_e$  and that the cells were able to repopulate the electrodes under these conditions (Figure 1C).

The efficiency of recovering the wounded electrode was quantified by AUC calculations as described in materials and methods (Figure 1D). SK-Mel-28 showed no migration in the presence of pH 6.0, while the mean AUC increased for increasing pH between pH 6.5 and pH 8.5 (Figure 1E).

To investigate the role of GPR4 in melanoma cell migration, we generated a GPR4 overexpressing cell line (see materials and methods as well as supplementary materials and methods). SK-Mel-28 WT cells were transfected with a GPR4-GFP construct that made the subcellular localization of the receptor visible by confocal fluorescence microscopy (Figure 2A). In SK-Mel-28\_GPR4 cells the GFP-receptor construct seems to be expressed at the cell membrane and at intracellular locations, possibly ER, Golgi and vesicles (see for comparison SK-Mel-28 expressing GFP only in Figure S1). qPCR analysis was performed to quantify the GPR4 overexpression relative to SK-Mel-28 WT cells (Figure 2B). Data revealed significant relative overexpression of GPR4 in SK-Mel-28\_GPR4 cells by a factor of  $2300 \pm 750$  (mean ± SEM of  $n = 6$  (WT)/8 (GPR4)). Additional Western Blot Analysis demonstrated a significant overexpression of GPR4 in SK-Mel-28\_GPR4 as compared to the control (Figure 2C,D).

With this GPR4 overexpression melanoma cell model, we performed the impedance-based electrical wounding and migration assay in the presence of different  $pH_e$  (Figure 3). The time courses of impedance before and after electrical wounding (indicated by an arrow) show that GPR4 overexpression affects the migration behaviour of SK-Mel-28 cells in a pH-dependent manner (Figure 3A–H). Neither SK-Mel-28 WT cells nor GPR4 overexpressing cells showed a significant recovery of impedance after wounding at  $pH_e$  6.0. Between  $pH_e$  6.5 and  $pH_e$  7.5 GPR4 overexpressing cells showed a faster recovery of impedance than compared to WT cells. After 30 h into the measurement the impedance levels of GPR4 overexpressing cells were higher than for WT cells. For  $pH_e$  8.0 and 8.5, this effect was less pronounced and the impedance values at the end of the measurement were similar or lower for SK-Mel-28\_GPR4 impedance values at the end of the measurement.

As the data set shown in Figure 3 is restricted to a small sample number for the sake of clarity, a quantitative AUC analysis of at least two additional data sets with two technical replicates each was performed (c.p. materials and methods). AUC quantification by AUC calculations from three independent measurements as shown in Figure 3A–H confirmed that the difference in AUC was significant for  $pH_e$  6.5–7.5 (Figure 3I–P). Results reflect an increased migration activity at these pH values for GPR4 overexpressing versus WT cells. At  $pH_e$  8.0 and 8.5 no significant difference in migration behaviour was detected by this assay. Results indicate that GPR4 enhances the migratory activity of SK-Mel-28 cells at pH between pH 6.5 and

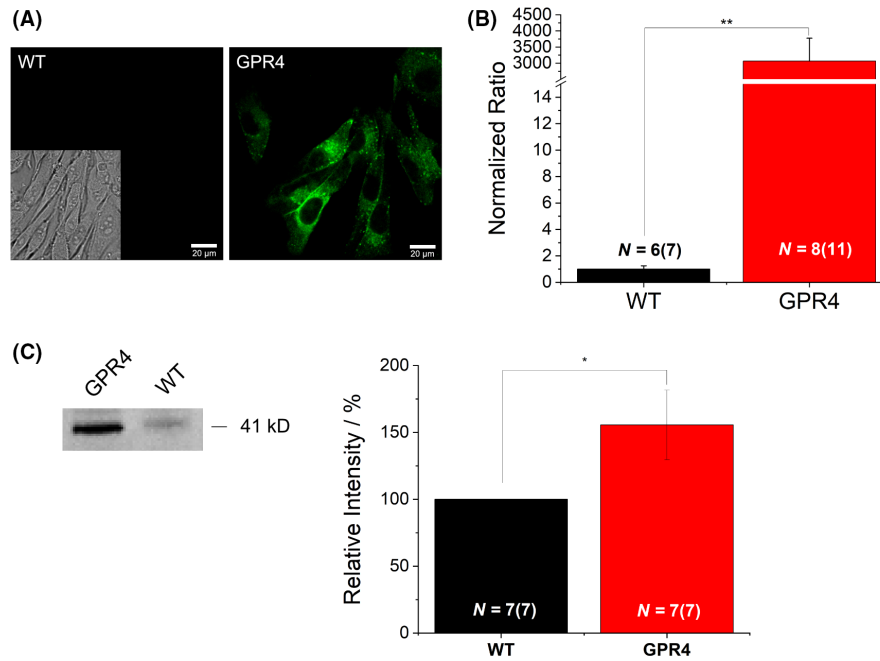


**FIGURE 2** Overexpression of GPR4 in SK-Mel-28. (A) Confocal fluorescence micrographs (CLSM) of (left) SK-Mel-28 WT cells and (right) SK-Mel-28 stably expressing the pH-GPCRs GPR4 (SK-Mel-28\_GPR4) at pH 7.5. Scale bar represents 20 μm. (B) Results of GPR4 mRNA quantification in SK-Mel-28 cells by qPCR. The figure shows the normalized ratio of GPR4 mRNA relative to β-actin mRNA for WT and for GPR4 overexpressing cells (SK-Mel-28\_GPR4). Values of mRNA relative to β-actin were normalized to WT and are shown as mean ± SEM for  $N = 6(7) - 8(11)$ . Normalized ratios are WT:  $1 \pm 0.2$ , GPR4:  $2300 \pm 750$ . (C) Western blot against GPR4 (left) and quantitative analysis of Western blots for GPR4 expression for GPR-4 overexpressing SK-Mel-28 (41 kD:  $160 \pm 30\%$ ) relative to WT (100%). Values are shown as mean ± SEM for  $N = 7(7)$ .

pH 7.5 and thus might play a role in  $pH_e$ -driven metastasis of melanoma in this pH range.

To confirm and complement the outcome of the impedance-based wounding and migration assay, a classical Boyden chamber assay was performed in two experimental layouts (Figure 4). The transwell inserts were either used uncoated or they were precoated with a stroma ECM surrogate (Matrigel) as an additional barrier for migration. Matrigel is a complex mixture of basement membrane components isolated from Engelbreth-Holm-Swarm (EHS) mouse sarcoma in a hydrogel matrix. To migrate through Matrigel, cells have to activate extracellular hydrolases that open the hydrogel structure for cell locomotion. Cells successfully reaching the other side of the filter membrane are not only considered motile but also invasive, as they express the enzymes necessary to get across the Matrigel layer. Moreover, the Boyden chamber assays use a chemottractant (serum) to initiate migration, whereas in the impedance-based assay cell migration is initiated by a sudden decrease in cell density, the accompanying loss of contact inhibition or secretion of autocrine factors. At pH 6.5 the overexpression of GPR4 had no impact on the chemotactic migration, as the cell count was insignificantly lower for GPR4 overexpressing cells (Figure 4A,B) compared to WT independent of the presence of Matrigel. So neither cell locomotion nor invasion was altered by the expression of GPR4. At pH 7.5 the GPR4 overexpressing SK-Mel-28 cells showed a significantly increased locomotion across porous membranes in the Boyden chamber assay (Figure 4C) in the absence of Matrigel. The invasion through the

Matrigel layer and subsequent migration through the pores of the filter was also slightly enhanced for GPR4 overexpressing SK-Mel-28 cells compared to SK-Mel-28 WT cells at this  $pH_e$ , the results were, however, not significant. In summary, the different migration assays performed in this study reveal a complex impact of GPR4 activation on cell migration/invasion. Whereas invasion is not affected at pH 6.5 and 7.5, the pure locomotion activity in the absence of Matrigel was higher at pH 7.5 compared to at pH 6.5. Similarly, the impedance-based migration assay that mirrors activation of cell migration (not invasion) due to tissue lesions in the absence of 3D ECM revealed an enhanced migration of the GPR4 overexpressing cells for pH between 6.5 and 7.5. Thus, the two assays reading primarily cell locomotion indicated an impact of GPR4 on cell migration. Invasive properties of the cells were, however, not affected by the GPR4-mediated signalling. The proliferation of SK-Mel-28 cells appears to be independent of pH, as an ATP assay only showed a slight but insignificantly higher luminescence for both, WT and GPR4 overexpressing cells at low  $pH_e$  (see Figure S2). Thus, the differences seen for GPR4 overexpressing versus WT cells in  $pH_e$ -dependent migration seem to be unaffected by proliferation.

## 4 | DISCUSSION

Recently published immunohistochemistry data indicate that malignant melanoma express pH-GPCRs at higher levels as compared

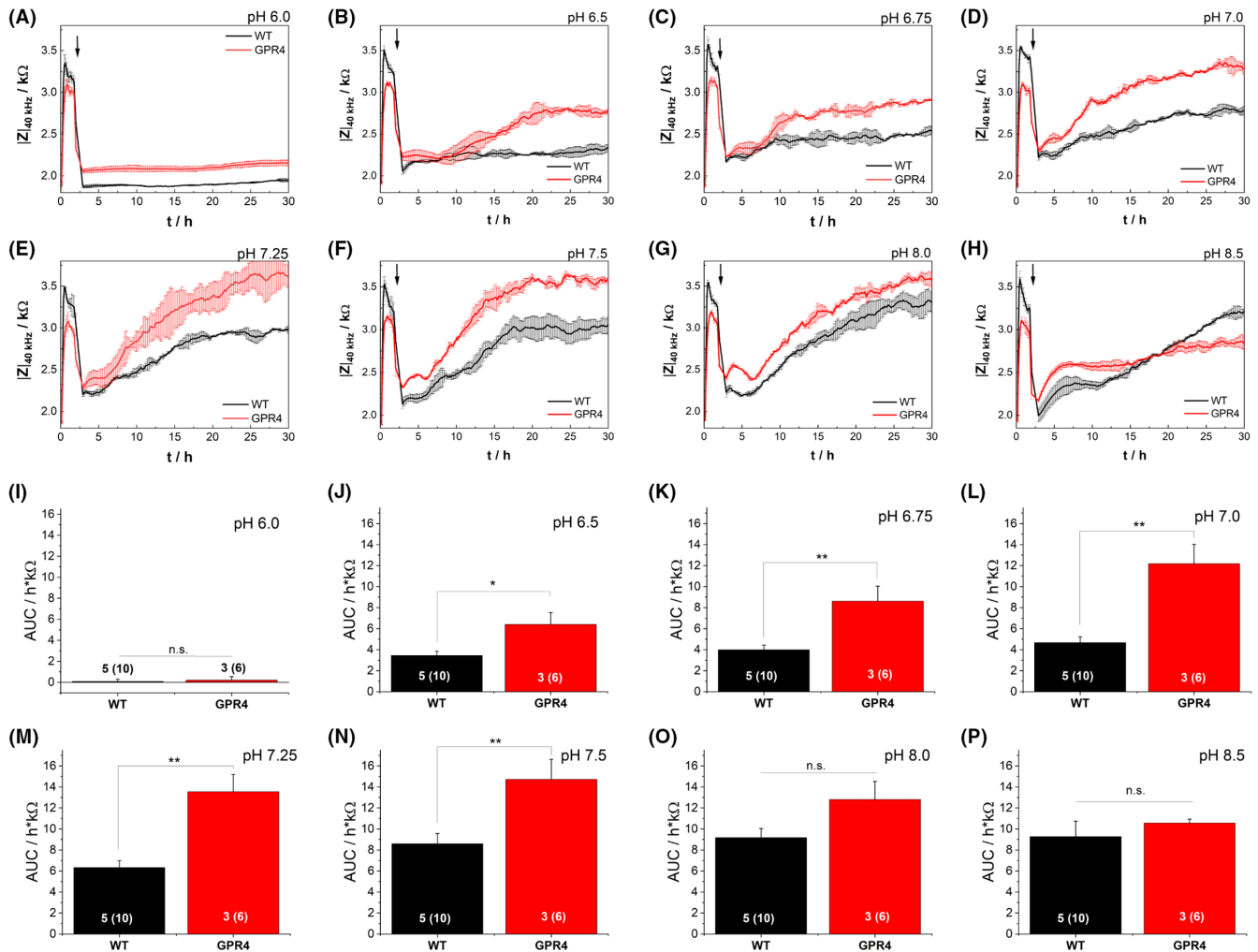


**FIGURE 3** Effect of GPR4 overexpression on SK-Mel-28 melanoma cell migration. (A–H) Typical time courses of impedance magnitude at 40kHz for SK-Mel-28\_GPR4 cells (GPR4) (red lines) compared to SK-Mel-28 wildtype (WT) (black lines) cells upon electric wounding in the presence of different  $\text{pH}_e$ . Data represent mean  $\pm$  SD of one typical experiment with two replicates per condition. (I–P) Quantitative area under the curve (AUC) analysis of at least three individual experiments conducted in duplicates per condition  $N = 3 (6) - 5 (10)$  shown as mean + SEM.

to benign nevi.<sup>32</sup> Especially GPR4 was shown to be frequently expressed at high levels in the dermal portion of malignant melanoma biopsies, which suggests that GPR4 could promote metastasis of melanoma. Eleven studies on cBioportal (<https://www.cbioportal.org/>) were analysed for mutation frequency of GPR4, which showed up to 8% mutations (half of these amplifications) in studies on metastatic melanoma (Figure S3). This goes to show that differences in GPR4 expression are quite frequent in MM.

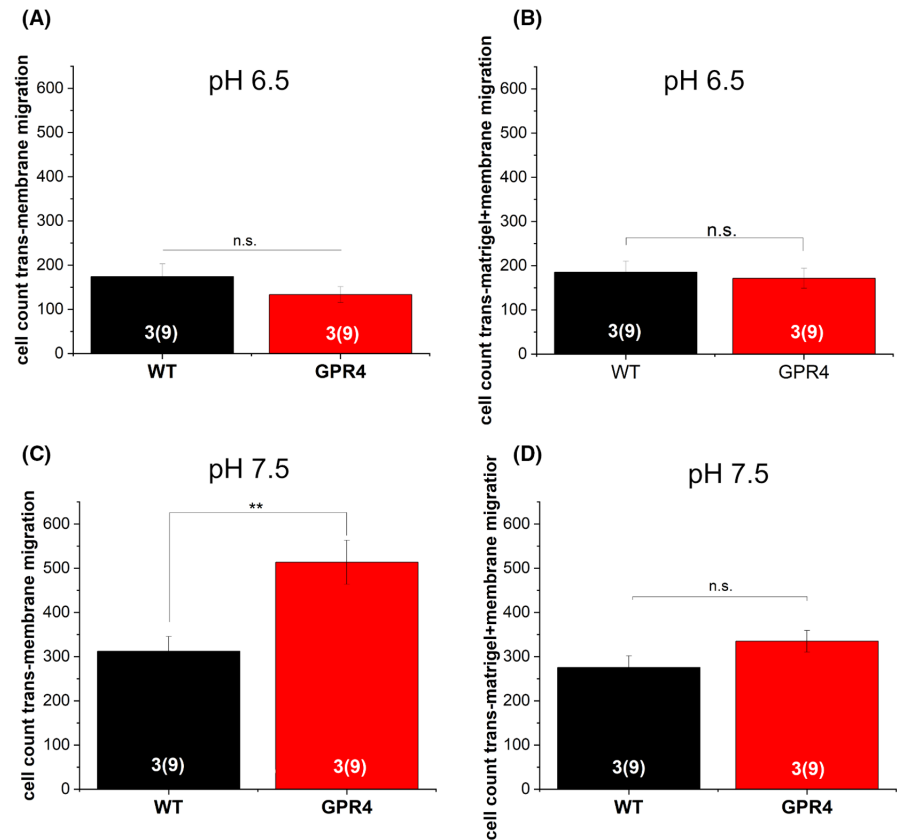
Therefore, we sought to investigate the role of GPR4 in the migration/invasion phenotype of SK-Mel-28 melanoma cells. We transfected SK-Mel-28 melanoma cells with a GPR4-GFP construct to be able to visualize receptor localization. The SK-Mel 28 have mutations in BRAF (c.1799T>A, p.V600E), p53 (c.434T>C, p.L145R), and CDK4 (c.70C>T, p.R24C), and these sites are not altered via GPR4 overexpression.<sup>37</sup> According to qPCR analyses the endogenous levels of GPR4 are relatively low in SK-Mel-28 melanoma cells compared to other dermal cell lines (see Figure S4). Like in other

studies at  $\text{pH} \sim 7.5$  the GFP-receptor construct was visible at the cell membrane as well as in intracellular compartments.<sup>38,39</sup>

Any discussion about cell migration, which is an umbrella term in cell biology, has to distinguish between cell locomotion (i.e. the ability of cells to change their local position) and cell invasion (i.e. the ability to penetrate the basement membrane and adjacent stroma ECM). It has been the key finding of this study, that cell locomotion is affected by overexpression of GPR4 in a  $\text{pH}_e$  range of 6.5–7.5 but invasion through a stroma ECM surrogate was not. Both, the impedance-based migration assay and the Boyden chamber studies in the absence of Matrigel reveal increased cell locomotion even though the modes of cell locomotion are very different. The impedance-based assay measures the closure of an in vitro lesion in an otherwise confluent cell monolayer which requires the removal of cell debris prior to wound closure. Moreover, cell locomotion is triggered by a sudden decrease of areal cell density and the associated signalling. The movement of the cells shows many aspects



**FIGURE 4** Migration of SK-Mel-28 cells stably transfected with GPR4 compared to SK-Mel-28 wildtype (WT) cells in a Boyden chamber at  $\text{pH}_e$  6.5 and  $\text{pH}_e$  7.5. (A, C) The Boyden chamber inserts only contained a porous membrane (8  $\mu\text{m}$  pores) (B, D) or were covered by an additional Matrigel layer. Cell count results are shown as mean  $\pm$  SEM for three individual experiments conducted in triplicates per condition ( $N = 3(9)$ ).



of collective cell migration. In the Boyden chamber assay in the absence of Matrigel, cells move towards a chemottractant (serum) which induces presumably a very different intracellular signalling and cell locomotion is clearly considered as single-cell locomotion. Despite these differences, both assays returned enhanced cell locomotion of GPR4 overexpressing melanoma cells compared to their wild strongly supporting a potential role of GPR4 for enhanced cell migration and a potential role in metastatic progression. So far, it is unknown whether ameboid or mesenchymal migration is impacted by GPR4 in melanoma. However, in some cancers mutant p53 results in an ameboid morphology and loss of p16 seem to lead to a mesenchymal morphology.<sup>40</sup>

A typical key feature of solid tumors is a  $\text{pH}_e$  gradient ranging from low  $\text{pH}_e$  at the center of the tumor tissue to almost normal or normal  $\text{pH}_e$  at the periphery of the tumor [4]. Even though acidic  $\text{pH}_e$  inhibits migration, that is, in the center of the tumor, the increased migratory potential at normal pH (~7.5) can enhance the dissemination and metastasis of cells at the edge of the tumor cells into surrounding tissue with physiological  $\text{pH}_e$ . Studies with B16 mouse melanoma cells have seen an inhibitory effect of GPR4-overexpression on migration.<sup>28</sup> However, this was only investigated for very low  $\text{pH}_e$ , which are only present in or in the vicinity of the tumor. In our study, melanoma cells with GPR4-overexpression that are exposed to rather normal extracellular  $\text{pH}_e$ , for example, in other tissues, show increased migration. The effect might play a major role in the seeding of these cells in other types of tissue. Furthermore, GPR4 also positively affects adhesion,<sup>13</sup> which was

not our focus in this series of experiments. Interestingly, this could even strengthen our results, because adhesion is a different process than migration and low  $\text{pH}_e$  might facilitate local tumor growth in GPR4-overexpressing melanoma.

The Boyden chamber assay in the presence of Matrigel did not show any significant impact of GPR4 overexpression. However, the assays read primarily cell invasion of extracellular matrices which requires the expression and activation of membrane-bound or extracellular hydrolases to open up a path for directed cell growth. Matrigel is a basement membrane ECM mixture produced by mouse tumor cells. It contains many factors, including laminin, collagen IV, heparan sulfate proteoglycan perlecan and nidogen/entactin.<sup>41</sup> The migration across dense basement membranes and adjacent stroma ECM usually requires matrix remodelling by the secretion of different proteases [4]. For example, a cAMP/EPAC signalling-dependent pathway that resulted in syndecan-2 translocation and heparan sulfate production was suggested as playing a central role in melanoma migration.<sup>42</sup> It is possible that neither the matrix composition nor the activity to produce necessary enzymes for matrix remodelling have significantly changed for SK-Mel\_GPR4 cells compared to WT cells, and therefore the impact of GPR4 on trans-Matrigel migration is negligible. The bottom line, GPR4 is only responsible for any change in cell locomotion but not for the infiltration of tissues and extracellular matrices underlying the dermal portion of the skin.

The pH range in which GPR4 is activated was reported to be pH 5.6–7.6.<sup>10–12</sup> The study by Ludwig et al.<sup>10</sup> measured a half-maximal

activation of cAMP formation by GPR4 in transiently transfected HEK293 cells at a pH of  $7.55 \pm 0.02$  (mean  $\pm$  SEM). Measurements of GPR4 activation using a recombinant BRET-based mini-G protein (mGp) assay in HEK293 cells resulted in half-maximal activation at pH  $7.1 \pm 0.029$  (mean  $\pm$  SEM).<sup>12</sup> A further study found half-maximal cAMP accumulation upon activation of WT GPR4 in HEK293 at pH  $7.4 \pm 0.043$  (mean  $\pm$  SEM).<sup>38</sup> In all three studies maximum activation of GPR4 was reached at around pH 6.3–6.5, while no significant activation was detected beyond pH 8.0,<sup>10,12,38</sup> which matches well with observations of this study.

GPR4 has been described to mainly activate the  $G_s$  pathway, although the involvement of  $G_{12/13}$  and  $G_{q/11}$  signalling is also considered.<sup>10,14,28,30,38,43</sup> Signalling pathways that are activated by cAMP play a critical role in cancer cell metabolism, growth and migration<sup>44,45</sup> and are described as being potentially relevant in the transformation of melanocytes into malignant melanoma.<sup>45,46</sup> Impaired cAMP signalling has been associated with an increased risk of melanoma, but the exact role of cAMP-dependent pathways in melanoma is not known yet and appears to be strongly dependent on the genetic background.<sup>46–48</sup> Studies indicate, that cAMP promotes melanoma cell migration and angiogenesis via activation of the protein “exchange protein activated by cAMP” (EPAC).<sup>46,47,49</sup> Application of a membrane permeable cAMP analog (8-pMeOPT) led to a significantly increased migration and rearrangement of the actin cytoskeleton in SK-Mel-2 melanoma cells.<sup>47</sup> According to a more recent study, the ectopic overexpression of GPR4 in murine B16F10 melanoma cells delayed cell spreading and affected focal adhesion localization and actin distribution, which points to alterations in cell mobility.<sup>28</sup> In stark contrast to the findings on GPR4 overexpressing SK-Mel-28 cells in this study, ectopic overexpression of GPR4 in B16F10 melanoma cells inhibited their migration, as assessed by a 2D scratch assay (pH 6.4–7.4) and Boyden chamber migration assays (pH 6.4–7.9 without Matrigel, pH 6.4–7.9 with Matrigel), and reduced their potential to form lung metastases in a mouse model.<sup>13</sup> The reason for the opposite results might be caused by the different genetic background of the murine B16F10 and human SK-Mel-28 melanoma cell models. More melanoma cell lines should be investigated before a final conclusion of the role of GPR4 in melanoma is justified. Interestingly, a model with GPR4-deficient mice showed significantly reduced growth and vascularization of 4T1 breast or CT26 colon tumor cells, which points to a tumor-promoting effect of GPR4 by angiogenesis.<sup>18</sup> Supporting this pro-angiogenic effect an overexpression of GPR4 in squamous cell carcinoma led to an enhanced vascularization under acidic conditions, likely via increased production of the pro-angiogenic factors IL6, IL8 and VEGF by these cells.<sup>27</sup>

It is also possible that the differential effects of GPR4 on B16 versus SKMEL28 may partially be due to the fact that B16 is the WT for BRAF, but SKMEL28 is BRAF mutant. The expression level of BRAF seems to positively correlate with that of GPR4 in melanoma. Also, GPR4 has been shown to constitutively suppress ERK1/2 activation.<sup>50</sup> It is unlikely that disruption of GPR4 enhances BRAFV600E tolerance by derepressing ERK1/2, as the disruption should in theory

exacerbate the cellular stress caused by BRAFV600E overexpression (which activates ERK1/2). Ko et al.<sup>51</sup> suggested that disruption of GPR4 may enhance BRAFV600E tolerance by attenuating cellular apoptosis through a mechanism that remains to be elucidated.

In other cancer cell models, the data also point towards a tumor-promoting effect of GPR4. The knockdown of GPR4 in HCT116 and HT29 colorectal cancer cell lines resulted in suppressed growth and significantly inhibited invasion.<sup>30</sup> GPR4 was upregulated in human colorectal cancer samples and correlated with poor outcome.<sup>30</sup> GPR4 was also found to be overexpressed in a significant portion of the breast, ovarian, colon, liver and kidney tumors.<sup>29</sup> However, a first online search at Survival Genie (<https://bbisr.shinyapps.winsh.ip.emory.edu/SurvivalGenie/>)<sup>52</sup> on the effect of high versus low GPR4-expression showed no difference in survival rates of metastatic melanoma patients (Figure S5).

Overexpression of GPR4 in NIH3T3 or HEK293 cells malignantly transformed the cells. In HEK293 cells GPR4 expression led to transcriptional activation of SRE and CRE promotor-driven genes, indicating potential involvement of  $G_s$  and  $G_{12/13}$  signalling and activation of a multitude of genes involved in proliferation and migration.<sup>29</sup> Indeed, NIH3T3 cells overexpressing GPR4 that were injected to mice led to increased tumor formation.<sup>29</sup>

In the 2D migration assay, the effect of GPR4 overexpression on migration was most pronounced between pH 6.75 and 7.5.

## 5 | CONCLUSION

Triggered by clinical evidence for overexpression of GPR4 in metastatic melanoma, this study addressed the impact of GPR4 on cell locomotion and cell invasion in an established melanoma in vitro model based on the SK Mel 28 cell line. Overexpression of GPR4 was compared to WT with respect to the cell migration phenotype using different cell migration assays. The experimental outcome suggests that GPR4 overexpression is responsible for enhanced cell motility leading to enhanced cell locomotion as long as no extracellular matrix barriers are present. However, GPR4 overexpression does not induce a more invasive phenotype in the sense of an enhanced ability to penetrate extracellular matrices. This study indicates that other external factors are required to induce this more invasive phenotype. Accordingly, GPR4 overexpression may not be solely responsible for metastatic progression in melanoma but it does affect one of its key hallmarks which is cell locomotion.

## AUTHOR CONTRIBUTIONS

*Conceptualization:* Judith Anthea Stolwijk and Stephan Schreml. *Investigation:* Judith Anthea Stolwijk, Susanne Wallner, Lisa Pütz, Judith Heider, Stefanie Michaelis, Julia Erl, Linda Frank and Barbara Goricnik. *Resources:* Stephan Schreml and Joachim Wegener; *Writing—original draft preparation:* Judith Anthea Stolwijk; *Writing—review and editing:* Judith Anthea Stolwijk, Stephan Schreml, Bernadett Kurz, Lisa Pütz, Mark Berneburg, Joachim Wegener and Frank Haubner. *Visualization:* Judith Anthea Stolwijk. *Supervision:*

Stephan Schreml, Judith Anthea Stolwijk and Joachim Wegener. *Project administration*: Stephan Schreml, Judith Anthea Stolwijk and Joachim Wegener. *Funding acquisition*: Stephan Schreml and Joachim Wegener. All authors have read and agreed to the published version of the manuscript.

## ACKNOWLEDGEMENTS

None. Open Access funding enabled and organized by Projekt DEAL.

## FUNDING INFORMATION

This research was funded by the German Research Foundation DFG, grants SCHR 1288/4-3, SCHR 1288/6-1 and WE 2721/7-3.

## CONFLICT OF INTEREST

The authors declare no conflict of interest.

## DATA AVAILABILITY STATEMENT

The data that support the findings of this study are available from the corresponding author upon reasonable request.

## ORCID

Stephan Schreml  <https://orcid.org/0000-0002-2820-1942>

## REFERENCES

- Bohme I, Bosserhoff AK. Acidic tumor microenvironment in human melanoma. *Pigment Cell Melanoma Res.* 2016;29:508-523.
- Davis LE, Shalin SC, Tackett AJ. Current state of melanoma diagnosis and treatment. *Cancer Biol Ther.* 2019;20:1366-1379.
- Naik PP. Cutaneous malignant melanoma: a review of early diagnosis and management. *World J Oncol.* 2021;12:7-19.
- Boedtker E, Pedersen SF. The acidic tumor microenvironment as a driver of cancer. *Annu Rev Physiol.* 2020;82:103-126.
- Webb BA, Chimenti M, Jacobson MP, Barber DL. Dysregulated pH: a perfect storm for cancer progression. *Nat Rev Cancer.* 2011;11:671-677.
- Neri D, Supuran CT. Interfering with pH regulation in tumours as a therapeutic strategy. *Nat Rev Drug Discov.* 2011;10:767-777.
- Weiss KT, Fante M, Kohl G, et al. Proton-sensing G protein-coupled receptors as regulators of cell proliferation and migration during tumor growth and wound healing. *Exp Dermatol.* 2017;26:127-132.
- Damaghi M, Wojtkowiak JW, Gillies RJ. pH sensing and regulation in cancer. *Front Physiol.* 2013;4:370.
- Justus CR, Dong L, Yang LV. Acidic tumor microenvironment and pH-sensing G protein-coupled receptors. *Front Physiol.* 2013;4:354.
- Ludwig MG, Vanek M, Guerini D, et al. Proton-sensing G-protein-coupled receptors. *Nature.* 2003;425:93-98.
- Sisignano M, Fischer MJM, Geisslinger G. Proton-sensing GPCRs in health and disease. *Cell.* 2021;10:2050.
- Rowe JB, Kapolka NJ, Taghon GJ, Morgan WM, Isom DG. The evolution and mechanism of GPCR proton sensing. *J Biol Chem.* 2021;296:100167.
- Castellone RD, Leffler NR, Dong L, Yang LV. Inhibition of tumor cell migration and metastasis by the proton-sensing GPR4 receptor. *Cancer Lett.* 2011;312:197-208.
- Chen A, Dong L, Leffler NR, Asch AS, Witte ON, Yang LV. Activation of GPR4 by acidosis increases endothelial cell adhesion through the cAMP/Epac pathway. *PLoS One.* 2011;6:e27586.
- Dong L, Li Z, Leffler NR, Asch AS, Chi JT, Yang LV. Acidosis activation of the proton-sensing GPR4 receptor stimulates vascular endothelial cell inflammatory responses revealed by transcriptome analysis. *PLoS One.* 2013;8:e61991.
- He XD, Tobo M, Mogi C, et al. Involvement of proton-sensing receptor TDAG8 in the anti-inflammatory actions of dexamethasone in peritoneal macrophages. *Biochem Biophys Res Commun.* 2011;415:627-631.
- Mogi C, Tobo M, Tomura H, et al. Involvement of proton-sensing TDAG8 in extracellular acidification-induced inhibition of proinflammatory cytokine production in peritoneal macrophages. *J Immunol.* 2009;182:3243-3251.
- Wyder L, Suply T, Ricoux B, et al. Reduced pathological angiogenesis and tumor growth in mice lacking GPR4, a proton sensing receptor. *Angiogenesis.* 2011;14:533-544.
- Li J, Guo B, Wang J, Cheng X, Xu Y, Sang J. Ovarian cancer G protein coupled receptor 1 suppresses cell migration of MCF7 breast cancer cells via a Galpha12/13-rho-Rac1 pathway. *J Mol Signal.* 2013;8:6.
- Ren J, Zhang L. Effects of ovarian cancer G protein coupled receptor 1 on the proliferation, migration, and adhesion of human ovarian cancer cells. *Chin Med J.* 2011;124:1327-1332.
- Singh LS, Berk M, Oates R, et al. Ovarian cancer G protein-coupled receptor 1, a new metastasis suppressor gene in prostate cancer. *J Natl Cancer Inst.* 2007;99:1313-1327.
- Yan L, Singh LS, Zhang L, Xu Y. Role of OGR1 in myeloid-derived cells in prostate cancer. *Oncogene.* 2014;33:157-164.
- Chen P, Zuo H, Xiong H, et al. Gpr132 sensing of lactate mediates tumor-macrophage interplay to promote breast cancer metastasis. *Proc Natl Acad Sci U S A.* 2017;114:580-585.
- Justus CR, Sanderlin EJ, Dong L, et al. Contextual tumor suppressor function of T cell death-associated gene 8 (TDAG8) in hematological malignancies. *J Transl Med.* 2017;15:204.
- Le LQ, Kabarowski JH, Wong S, Nguyen K, Gambhir SS, Witte ON. Positron emission tomography imaging analysis of G2A as a negative modifier of lymphoid leukemogenesis initiated by the BCR-ABL oncogene. *Cancer Cell.* 2002;1:381-391.
- Li Z, Dong L, Dean E, Yang LV. Acidosis decreases c-Myc oncogene expression in human lymphoma cells: a role for the proton-sensing G protein-coupled receptor TDAG8. *Int J Mol Sci.* 2013;14:20236-20255.
- Jing Z, Xu H, Chen X, et al. The proton-sensing G-protein coupled receptor GPR4 promotes angiogenesis in head and neck cancer. *PLoS One.* 2016;11:e0152789.
- Justus CR, Yang LV. GPR4 decreases B16F10 melanoma cell spreading and regulates focal adhesion dynamics through the G13/rho signaling pathway. *Exp Cell Res.* 2015;334:100-113.
- Sin WC, Zhang Y, Zhong W, et al. G protein-coupled receptors GPR4 and TDAG8 are oncogenic and overexpressed in human cancers. *Oncogene.* 2004;23:6299-6303.
- Yu M, Cui R, Huang Y, Luo Y, Qin S, Zhong M. Increased proton-sensing receptor GPR4 signalling promotes colorectal cancer progression by activating the hippo pathway. *EBioMedicine.* 2019;48:264-276.
- Zhang Y, Feng Y, Justus CR, et al. Comparative study of 3D morphology and functions on genetically engineered mouse melanoma cells. *Integr Biol (Camb).* 2012;4:1428-1436.
- Klatt W, Wallner S, Brochhausen C, Stolwijk JA, Schreml S. Expression profiles of proton-sensing G-protein coupled receptors in common skin tumors. *Sci Rep.* 2020;10:15327.
- Nassios A, Wallner S, Haferkamp S, Klingelhoffer C, Brochhausen C, Schreml S. Expression of proton-sensing G-protein-coupled receptors in selected skin tumors. *Exp Dermatol.* 2019;28:66-71.
- Wegener J, Keese CR, Gaever I. Electric cell-substrate impedance sensing (ECIS) as a noninvasive means to monitor the kinetics of cell spreading to artificial surfaces. *Exp Cell Res.* 2000;259:158-166.

35. Giaever I, Keese CR. Monitoring fibroblast behavior in tissue culture with an applied electric field. *Proc Natl Acad Sci U S A*. 1984;81:3761-3764.
36. Stolwijk JA, Wegener J. Impedance-based assays along the life span of adherent mammalian cells In vitro: from initial adhesion to cell death. In: Wegener J, ed. *Label-Free Monitoring of Cells In Vitro*. Springer International Publishing; 2019:1-75.
37. Rossi S, Cordella M, Tabolacci C, et al. TNF-alpha and metalloproteases as key players in melanoma cells aggressiveness. *J Exp Clin Cancer Res*. 2018;37:326.
38. Liu JP, Nakakura T, Tomura H, et al. Each one of certain histidine residues in G-protein-coupled receptor GPR4 is critical for extracellular proton-induced stimulation of multiple G-protein-signaling pathways. *Pharmacol Res*. 2010;61:499-505.
39. Radu CG, Nijagal A, McLaughlin J, Wang L, Witte ON. Differential proton sensitivity of related G protein-coupled receptors T cell death-associated gene 8 and G2A expressed in immune cells. *Proc Natl Acad Sci U S A*. 2005;102:1632-1637.
40. Arbiser JL, Bonner MY, Gilbert LC. Targeting the duality of cancer. *NPJ Precis Oncol*. 2017;1:23.
41. Kleinman HK, Martin GR. Matrigel: basement membrane matrix with biological activity. *Semin Cancer Biol*. 2005;15:378-386.
42. Baljinnam E, Iwatsubo K, Kurotani R, et al. Epac increases melanoma cell migration by a heparan sulfate-related mechanism. *Am J Physiol Cell Physiol*. 2009;297:C802-C813.
43. Tobo M, Tomura H, Mogi C, et al. Previously postulated "ligand-independent" signaling of GPR4 is mediated through proton-sensing mechanisms. *Cell Signal*. 2007;19:1745-1753.
44. Wehbe N, Slika H, Mesmar J, et al. The role of Epac in cancer progression. *Int J Mol Sci*. 2020;21:6489.
45. Zhang H, Kong Q, Wang J, Jiang Y, Hua H. Complex roles of cAMP-PKA-CREB signaling in cancer. *Exp Hematol Oncol*. 2020;9:32.
46. Bang J, Zippin JH. Cyclic adenosine monophosphate (cAMP) signaling in melanocyte pigmentation and melanomagenesis. *Pigment Cell Melanoma Res*. 2021;34:28-43.
47. Baljinnam E, De Lorenzo MS, Xie LH, et al. Exchange protein directly activated by cyclic AMP increases melanoma cell migration by a Ca<sup>2+</sup>-dependent mechanism. *Cancer Res*. 2010;70:5607-5617.
48. Rodriguez CI, Castro-Perez E, Prabhakar K, et al. EPAC-RAP1 Axis-mediated switch in the response of primary and metastatic melanoma to cyclic AMP. *Mol Cancer Res*. 2017;15:1792-1802.
49. Baljinnam E, Umemura M, Chuang C, et al. Epac1 increases migration of endothelial cells and melanoma cells via FGF2-mediated paracrine signaling. *Pigment Cell Melanoma Res*. 2014;27:611-620.
50. Bektas M, Barak LS, Jolly PS, et al. The G protein-coupled receptor GPR4 suppresses ERK activation in a ligand-independent manner. *Biochemistry*. 2003;42:12181-12191.
51. Ko T, Sharma R, Li S. Genome-wide screening identifies novel genes implicated in cellular sensitivity to BRAF(V600E) expression. *Oncogene*. 2020;39:723-738.
52. Dwivedi B, Mumme H, Satpathy S, Bhasin SS, Bhasin M. Survival genie, a web platform for survival analysis across pediatric and adult cancers. *Sci Rep*. 2022;12:3069.

## SUPPORTING INFORMATION

Additional supporting information can be found online in the Supporting Information section at the end of this article.

**Figure S1.** (A) Migration of SK-Mel-28 wild type cells (WT) and SK-Mel-28 cells 72h after transient transfection with pCMV6-AC-GFP control vector (pCMV) at pH 7.5. The transfection with control vector alone did not lead to significant differences in cell migration of SKMel28 as measured via the impedance-based migration assay (see methods). Data are shown as mean  $\pm$  SD for n = 3. (B) Confocal fluorescence micrograph of SK-Mel-28 cells transfected with pCMV6-AC-GFP control vector (pCMV) and compared to SK-Mel-28 wild type cells (WT) and SK-Mel-28 cells 28 stably expressing GPR4 (SK-Mel-28\_GPR4).

**Figure S2.** Metabolic activity of SK-Mel-28 WT and SK-Mel-28\_GPR4 cells at different pH values.

**Figure S3.** Mutation frequency of GPR4 in melanoma. 11 studies were assessed on cBioportal (<https://www.cbioportal.org/>).

**Figure S4.** Expression profiles of GPR4 in different skin cell lines on mRNA level.

**Figure S5.** GPR4 expression and survival according to Survival Genie.

**How to cite this article:** Stolwijk JA, Wallner S, Heider J, et al. GPR4 in the pH-dependent migration of melanoma cells in the tumor microenvironment. *Exp Dermatol*. 2023;32:479-490. doi:[10.1111/exd.14735](https://doi.org/10.1111/exd.14735)